Hippocampal neurogenesis requires cell autonomous thyroid hormone signaling

Hippocampal neurogenesis requires cell autonomous thyroid hormone signalling

Steffen Mayerl[1], Heike Heuer [2], and Charles ffrench-Constant[1]

[1]MRC Centre for Regenerative Medicine, University of Edinburgh, United Kingdom
[2]University of Duisburg-Essen, University Hospital Essen, Dept. of Endocrinology, Germany

Corresponding author: Steffen Mayerl, PhD

MRC Centre for Regenerative Medicine

5 Little France Drive

Edinburgh, EH16 4UU, UK

Phone: +441316519558

Email: smayerl@exseed.ed.ac.uk

Abbreviated title: Mct8 deficiency impairs adult hippocampal neurogenesis

Keywords: Adult hippocampal neurogenesis, thyroid hormone, T3, T4, Slc16a2, MCT8, neuroblasts, P27KIP1

Summary

Adult hippocampal neurogenesis is strongly dependent on thyroid hormone (TH). Whether TH signalling regulates this process in a cell-autonomous or non-autonomous manner remains unknown. To answer this question, we used global and conditional knock-outs of the TH transporter monocarboxylate transporter 8 (MCT8), having first employed FACS and immunohistochemistry to demonstrate that MCT8 is the only TH transporter expressed on neuroblasts and adult slice cultures to confirm a necessary role for Mct8 in neurogenesis. Both mice with a global deletion or an adult neural stem cell-specific deletion of MCT8 showed decreased expression of the cell-cycle inhibitor P27KIP1, reduced differentiation of neuroblasts and impaired generation of new granule cells neurons, with global knock-out mice also showing enhanced neuroblast proliferation. Together, our results reveal a cell-autonomous role for TH signalling in adult hippocampal neurogenesis alongside non-cell autonomous effects on cell proliferation earlier in the lineage.

Introduction

Adult hippocampal neurogenesis is a highly orchestrated process with cells passing through distinct stages to generate granule cell neurons (GCNs) throughout life (Beckervordersandforth et al., 2015; Kempermann et al., 2004; Remaud et al., 2014). This process is initiated from neural stem cells (NSCs) in the subgranular zone (SGZ) that cycle between quiescence and an activated state in which they generate transiently amplifying precursors (TAPs) from which new postmitotic neurones are formed via an intermediate neuroblast (NB) state. These newly formed neurons eventually integrate into the existing dentate gyrus granule cell network thereby creating new connections that contribute to CNS plasticity.

A link between hippocampal neurogenesis and cognitive function is well-established and adult-onset hypothyroidism is known to result in cognitive perturbations such as learning and memory deficits (Correia et al., 2009; Miller et al., 2006; Osterweil et al., 1992; Remaud et al., 2014). In light of this, a number of studies have investigated if TH deficiency impairs the hippocampal neurogenic process. These studies have consistently demonstrated an effect on progenitor differentiation and the generation of neurons, but no consistent effects earlier in the lineage on NSC behaviour (Ambrogini et al., 2005; Desouza et al., 2005; Montero-Pedrazuela et al., 2006). However, a key question that remains unanswered is whether this effect results from a cell autonomous requirement for TH signalling within the hippocampal lineage or from an indirect, non-cell autonomous effect resulting from TH function in supporting glial and other cell types. Addressing this is important to identify the necessary cellular targets for therapies designed to treat age-related cognitive decline based on modulated TH signalling.

One strategy to address this question is to identify essential components of the TH signalling pathway selectively expressed in NBs and then compare the effects of global and conditional knock-outs of these components. The latter will reveal only cell autonomous effects, while the former will reveal both cell and non-cell autonomous effects. By examining the cellular expression pattern of components of the TH signalling pathway throughout the

adult hippocampal neurogenic program we identified such a component, the TH transporter MCT8. Transgenic mice lacking MCT8 either globally or just in the hippocampal neurogenic lineage both showed impaired differentiation of NBs and a reduced formation of new GCNs in the adult hippocampus. This impairment is associated with an improper regulation of the cell cycle inhibitor P27KIP1 in neural progenitors. We conclude that the effect of TH on the generation of neurons from NBs is cell-autonomous and that MCT8 is a critical gate-keeper for this step of hippocampal neurogenesis.

Results

Differential expression of TH signalling components within the hippocampal neurogenic lineage

TH signalling in the CNS is regulated at several levels. First, TH transporters such as the L-type amino acid transporters (LAT) 1 and 2, organic anion transporting polypeptide (OATP) 1C1 and monocarboxylate transporters (MCT) 8 and 10 are mandatory for TH transmembrane passage across the blood-brain-barrier (BBB) and cellular TH uptake (Bernal et al., 2015; Heuer and Visser, 2013). Second, intracellular iodothyronine deiodinases (DIO) then either activate (DIO2) or inactivate TH (DIO3) (Bianco et al., 2002). Third, μ-Cristallin (CRYM), a cytosolic TH binding protein, can regulate intracellular TH levels (Suzuki et al., 2007). Fourth, nuclear TH receptors (TRs) encompassing the ligand binding isoforms TRα1, TRβ1 and TRβ2 as well as non-ligand binding isoforms like TRα2 regulate gene expression in response to TH (Flamant and Gauthier, 2013; Koenig et al., 1989). Last, co-activators or co-repressors are recruited to TR isoforms, including NCOR (nuclear receptor corepressor; NCOR1) and SMRT (silencing mediator of retinoid and thyroid hormone receptors; NCOR2) (Astapova and Hollenberg, 2013).

To unravel the temporal expression pattern of these TH signalling components in the adult mouse hippocampus and identify any selectively expressed in NBs, we micro-dissected and dissociated dentate gyri for FACS. We used intracellular markers to isolate different progenitor/neuronal populations that develop in sequence within the hippocampal neurogenic lineage (Kempermann et al., 2004) (Fig.1A). The first cell population comprises NSCs that are located in the SGZ of the dentate gyrus, extend a radial process into the molecular layer and are positive for glia fibrillary acidic protein (GFAP), SRY-Box 2 (SOX2) and NESTIN. The second population encompasses TAPs (intermediate progenitors; type 2a and type 2b progenitors) which express the transcription factor T-box brain protein 2 (TBR2) and are generated by asymmetrical division of activated NSCs. This population can be subdivided by

expression of the neuronal differentiation-promoting factor PROX1 (Prospero Homeobox 1) and the immature neuronal marker Doublecortin (DCX) in type 2b progenitors. Cells of the third population, DCX+ type 3 NBs, develop a vertical process whilst exiting the cell cycle to generate, fourth, immature post-mitotic neurons (INs) which are characterized by transient expression of the Calcium-binding protein Calretinin (CR). Finally, the fifth population comprises GCNs in which Dcx and CR expression cease and Calbindin (CB) expression is initiated.

Using forward and side scatter, we separated cells (P1; 2.1-8.0%) from debris and selected single cells (P2; 94.9-98.9%) (Fig.S1A). Single cells viable before fixation were identified based on a low intensity of a fixable live/dead cell stain (P3; 38.4-53.4%). From those cells, a TBR2+ population was isolated (0.6-2.3%) (Fig.S1B). The TBR2- population (P4) was then subdivided into a DCX- and a DCX+ population (4.1-7.8%). The latter was then sorted into CR- NBs (51.1-92.4%) and into CR+ INs (5.9-42.6%). In a second sorting strategy, CB+ GCNs (5.5-21.3%) were isolated from live cells (P3) (Fig.S1C). From the CB- population (P4) NESTIN+/GFAP+ NSCs were sorted (1.1-5.2%). All other cells were collected for RIN value determination. To preserve RNA integrity, we performed staining and sorting steps at low temperatures and in the presence of RNase inhibitor. As shown in Fig.S1D comparing the RIN value of a fixed sample, a fixed/stained sample and cells undergoing the staining/sorting procedure, a RIN value of 7.0 or higher was reached with our measures.

We then performed qPCR on isolated populations after mRNA amplification. To validate the identity of the isolated cell populations, neurogenic marker expression was analysed (Fig.1B). The stem cell marker *Hes5* (Beckervordersandforth et al., 2015) was strongly expressed in NSCs. As expected, we found high *Dcx* mRNA expression in TAPs, NBs and INs. *Prox1* transcript was expressed in NB, IN and GCN samples. *NeuN* mRNA, though detectable in TAP and NB, was highly enriched in GCN samples. A NSC, NB and GCN sample were also used for RT-PCR (Fig.S1E). *Dcx* was again enriched in the NB population, while the lineage marker *Prox1* was found in both NBs and GCNs.

Next, we assessed the mRNA expression profile of TH signalling components. Within the TH transporters (Fig.1C), we observed *Mct8* transcripts primarily in NBs and GCNs while *Mct10* mRNA was enriched in mature neurons. *Lat1* and *Lat2* expression was detected in NSCs and TAPs, whereas only *Lat2* was further enriched in GCNs. Analysis of TR expression profiles revealed *Trα1*, *Trα2*, *Trβ1* and *Trβ2* transcripts in the hippocampal lineage (Fig.1D). While both *Trα* isoforms and *Trβ1* mRNAs were predominantly expressed in NSC, NB and GCN populations, *Trβ2* transcript levels were down-regulated upon neuronal maturation. Finally, *Crym*, *Dio3*, *Ncor* and *Smrt* exhibited a similar profile of transcripts with peaks in NB and GCN stages (Fig.1E) matching the expression of *Mct8*, *Trα1* and *Trα2*. Of note, *Oatp1c1*, *Dio1* and *Dio2* transcripts were not detected in the analysed cell populations.

To complement our qPCR analysis, we performed immunofluorescence studies using perfusion-fixed brain cryosections from 2-month-old animals and commercially available antibodies against DIO3, LAT1, LAT2, MCT8 and MCT10 in combination with cell-type specific markers. (Fig.2). In contrast to our qPCR results LAT1 co-localized only with the endothelial cell marker CD31/PECAM-1 throughout the dentate gyrus (Fig.S2) while none of the proteins above could be detected in GFAP+/SOX2+ NSCs (Fig.2A). No co-localisation with the proliferation marker MCM2 present in activated NSCs, TAPs and cycling NBs was observed for any component except MCT8, which was found in a specific subset of MCM2+ cells also expressing DCX (Fig.2B). By employing a triple staining protocol, we observed strong expression of MCT8 protein in DCX+/CR- NBs and in DCX+/CR+ INs (Fig.2A) while none of the other proteins showed detectable expression at this stage. In agreement with our qPCR results, CB+ GCNs were positive for DIO3, LAT2, MCT8, and MCT10 protein. Whereas MCT8 and MCT10 exhibited equal expression throughout the granule cell layer, an asymmetrical pattern was found for DIO3 and LAT2 with stronger signals in the region contacting the molecular layer of the hippocampus (Fig.2C). We conclude that MCT8 is present in NBs, while later stages of the lineage contain a wider range of transporters. As TH transporters are essential for TH signalling, this finding identifies MCT8 as a possible target for our global and

conditional knock-out strategy to define the cell autonomy of TH signalling during the generation of neurons from NBs.

Inhibition of MCT8 reduces the formation of new neurons in adult hippocampal slices

Before generating transgenic mice, we sought to confirm a functional role for MCT8 in hippocampal neurogenesis using commercially available inhibitors in vitro. For that purpose, we established a protocol to maintain adult hippocampal slices for at least three weeks by combining different published protocols (Kim et al., 2013; Kleine Borgmann et al., 2013) and adding Indomethacin for its protective effects on neurogenesis *in vivo* and *ex vivo* (Gerlach et al., 2016; Melo-Salas et al., 2018). As a readout, we performed EdU tracing studies together with KI67 labelling to quantify progenitor proliferation, DCX labelling to quantify type 2b progenitors, NBs and INs and NEUN staining for neurons (Fig.3A).

Incubation with the MCT8-specific inhibitor Silychristin (Johannes et al., 2016) for 24 h did not alter proliferation in the SGZ (Fig.S3A) or the number of EdU+ and KI67+/EdU+ cells (Fig.3B and C). By 7 days in culture a trend towards decreased formation (EdU+, Fig.3D) and proliferation (KI67+/EdU+, Fig.S3A) of DCX+ cells in Silychristin-treated slices was seen, while longer incubation with the inhibitor resulted in a significant reduction of newly formed neurons (NEUN+/EdU+) after 21 days (Fig.3E). By contrast, treatment of hippocampal slices with the LAT inhibitor BCH (Ritchie et al., 1999; Ritchie et al., 2003) or the deiodinase inhibitor iopanoic acid (Dentice et al., 2013) had no effect on proliferation or NB and neuron formation (Fig.S3B and C). These inhibitor studies point to a crucial role of MCT8 during later stages of hippocampal neurogenesis.

Absence of MCT8 in vivo *compromises adult hippocampal neurogenesis*

Having confirmed a functional role for MCT8 in vitro, we assessed the consequences of global inactivation of MCT8 in vivo. At the age of 2 months, overall NSC numbers (defined

as GFAP+/SOX2+ cells extending a radial process into the granule cell layer) were the same in MCT8ko and Wt littermates. However, NSC activation was impaired in MCT8ko mice as significantly fewer NSCs were labelled by the proliferation marker KI67 (Fig.4A). Total numbers of KI67+ progenitors and the density of KI67+/DCX+ type 2b and type 3 progenitors were similar between the genotypes (Fig.4B). Likewise, no difference in the number of TBR2+ TAPs (Fig.S4A), cleaved CASPASE3+ apoptotic cells (Fig.S4B) and DCX+/CR- NBs (Fig.4C) could be observed. In contrast, a significantly reduced number of DCX+/CR+ INs was found in the MCT8ko SGZ (Fig.4C) pointing to impaired differentiation.

To explore the dynamics of neurogenesis further, we performed EdU label-retention studies. We injected 2-month-old mice with EdU and followed the formation of progenitor cells and neurons by NSCs in the hippocampus (Fig.4D) either at day 3 post injection (3 dpi) to examine the level of proliferation within each population or 28 dpi to quantify the number of labelled cells that are fully differentiated. At 3 dpi, we detected significantly more EdU labelled KI67+/DCX+ progenitors and DCX+/CR- NBs in MCT8ko mice compared to Wt littermates (Fig.4E and 4F respectively) whereas numbers of DCX+/CR+/EdU+ newly formed INs were not different (Fig.4F). At 28 dpi, significantly fewer EdU+/CB+ GCNs were seen in MCT8ko mice (Fig.4G) demonstrating that dividing NBs exhibit differentiation impairments in the absence of MCT8.

Hippocampal neurogenesis is highly active in young animals and rapidly declines with age, being already greatly compromised around half a year of age (Ben Abdallah et al., 2010; Kuhn et al., 2018). We wondered if the deficits resulting from loss of MCT8 are also observed at older ages when the number of cells transitioning from NB to neuron populations is reduced. To address this, we repeated our analysis at 6 months using the same EdU injection paradigm as in Fig.4D. At this age, MCT8ko mice exhibited a slight but significantly increased density of GFAP+/SOX2+ cells with a radial process in the SGZ, while similar numbers of NSCs were labelled with KI67 (Fig.5A). No differences were observed in the number of TBR2+ TAPs (Fig.S5A), cleaved CASPASE3+ apoptotic cells (Fig.S5B) or the total number of KI67+ cells. While the increase in KI67+/DCX+ cells did not reach statistical significance (Fig.5B), the

number of DCX+/CR- cells in the SGZ (comprising NBs and type 2b cells) was almost doubled in MCT8ko mice (Fig.5C). In contrast, MCT8ko mice demonstrated a severely reduced formation of new GCNs (CB+/EdU+) when assessed at 28 dpi (Fig.5D). We conclude that the deficit in neuron differentiation is also present in older animals despite the overall reduction in neurogenesis.

As a second approach to follow the progeny of dividing NSCs, we employed a stable labelling strategy by generating Wt and MCT8ko mice expressing a *Nestin-CreERT2* construct and a *tdTomato* reporter (hereafter *Rfp*) (Fig.5E). Following 5 consecutive days of tamoxifen treatment at the age of 4 weeks, mice were kept for 5 months before analysis, so matching the 6 month-time point used in the EdU analysis above. A similar absolute number of NSCs were labelled in both genotypes, though their relative contribution to all RFP+ cells was significantly higher in MCT8ko mice (Fig.5F). Despite this, and in agreement with our EdU incorporation studies, the relative number of NSC-derived RFP+/CB+ cells amongst all RFP+ cells was significantly reduced in MCT8ko mice. Together, our experiments using different labelling techniques and ages confirm that the absence of MCT8 and thus the loss of TH transporter activity in NBs inhibits the generation of new GCNs in the dentate gyrus.

The deficit in neuron formation caused by MCT8 loss is cell-autonomous

These deficits in neurogenesis may result from cell-autonomous effects of MCT8 deletion in hippocampal NBs. Alternatively, the well-described endocrine alterations following global loss of MCT8 such as high serum T3 and low serum T4 levels and/or impaired transport of T3 across the blood-brain barrier (BBB) that in turn causes a mild central TH deficiency (Ceballos et al., 2009; Trajkovic et al., 2007) may impact NB differentiation and GCN formation. To distinguish between these possibilities, we generated a mouse model with specific deletion of MCT8 in the adult neurogenic lineage (Fig.6A). To this end, *Mct8*+/fl females were mated with males heterozygous for the *Nestin-CreERT2* allele and homozygous for a *tdTomato* reporter allele (hereafter *Rfp*) (Fig.6A). *Mct8+/y,Nestin-CreERT2/+,Rfp/+* (control) and

Mct8fl/y,Nestin-CreERT2/+,Rfp/+ (MCT8-NSCko) mice were used. Tamoxifen-induced Cre-activation at 1 month of age resulted in RFP expression and deletion of MCT8 in MCT8-NSCko animals in adult NSCs and thus the neurogenic lineages only as confirmed by the loss of MCT8 expression in RFP+ neurons in MCT8-NSCko mice (Fig.S6A). All analyses were performed 5 months later to match the 6-month time point of global MCT8ko mice which showed GCN formation impairments and higher NB numbers. Again, we corrected our analysis for differences between individual animals by normalizing cell counts to the overall number of RFP+ cells. We found no differences in the percentage of RFP+ NSCs (Fig.6B), activated NSCs (GFAP+/RFP+/KI67+/radial process; Fig.6C), proliferating cells (KI67+/RFP+), proliferating type 2b cells/NBs (DCX+/KI67+/RFP+) (Fig.6D), TBR2+/RFP+ TAPs (Fig.S6B) and apoptotic cells (CASPASE3+/RFP+; Fig.6E). In contrast to age-matched global MCT8ko mice where NB numbers were increased, we detected a similar number of NBs (DCX+/CR-/RFP+) in MCT8-NSCko and controls at 6 months of age alongside a trend towards fewer INs (DCX+/CR+/RFP+) (Fig.6F). As in global MCT8ko mice, however, the relative number of CB+/RFP+ GCNs was significantly decreased in MCT8-NSCko (Fig.6G), confirming a cell-autonomous role of MCT8 within the hippocampal neurogenic lineage.

Expression of the cell cycle inhibitor P27KIP1 is impaired in MCT8 deficiency

One mechanism by which TH induces differentiation is by suppression of the cell cycle (Remaud et al., 2014), with direct regulation of cell cycle inhibitors such as Cyclin-dependent kinase inhibitor 1B (CDKN1B; P27KIP1) (Garcia-Silva et al., 2002; Holsberger et al., 2003). To examine this mechanism in the hippocampal neurogenic lineage, we quantified P27KIP1 levels in DCX+/CR- NBs and DCX+/CR+ INs in 2-month-old Wt and MCT8ko mice (Fig.7A). We discovered significantly reduced P27 fluorescence intensities in both cell populations in MCT8ko animals and replicated this finding in both 6-month-old MCT8ko mice (Fig.7B), and 6 months old MCT8-NSCko mice (Fig.7C). As the CIP/KIP family of cell cycle/CDK inhibitors comprises two more members, P21CIP1/WAF1 and P57KIP2, we assessed their expression

in 2 and 6 months old Wt and MCT8ko mice, but failed to observe differences in P21 (Fig.7D and E respectively) and P57 (Fig.7F and G respectively) immunofluorescence levels. Likewise, *p27kip1/Dcx* transcript ratios were reduced in micro-dissected dentate gyri from 6-month-old MCT8ko mice while *p57* mRNA levels were not different (Fig.S7). In sum, our results show a specific decrease in P27KIP1 following loss of MCT8 in the hippocampal neurogenic lineage, which likely underlies the impaired differentiation capacities in MCT8 deficiency.

Discussion

Patients with adult-onset hypothyroidism show specific defects in hippocampal memory function and a decreased hippocampal volume (Cooke et al., 2014; Correia et al., 2009; Ittermann et al., 2018). These clinical findings may be explained by a profound impact of TH on hippocampal neurogenesis, a process imperative for learning and memory, as animal experiments have confirmed that TH deficiency delays neuronal differentiation and perturbs the birth of new GCN in the adult hippocampus (Ambrogini et al., 2005; Desouza et al., 2005; Montero-Pedrazuela et al., 2006). However, the widespread systemic effects of TH deficiency make it impossible from these experiments using globally hypothyroid animals to resolve the key question if TH signalling impairs neuroblast differentiation cell-autonomously. Here, we demonstrate such a cell-autonomous effect by using a conditional knock-out strategy following a comprehensive analysis of the cell-specific repertoire of TH transporters, receptors, and metabolizing enzymes during hippocampal neurogenesis. A combination of FACS and qPCR allowed us to analyse distinct cell populations within the neurogenic program. With this approach, we could confirm the presence of *Trα*, *Trβ1* and *Trβ2* transcripts in cycling progenitors and GCNs as well as *Trα1* expression in DCX+ progenitors as described before (Desouza et al., 2005; Kapoor et al., 2010). We also demonstrated the presence of DIO3 and the TH transporters LAT2, MCT8, and MCT10 in GCNs. Critically, however, of all TH transporters analysed only MCT8 was found to be expressed in NBs at both the mRNA and protein level, suggesting a distinct function within the TH-regulated neurogenic program and enabling its manipulation as a means of addressing the central question of this study.

To our knowledge, this is the first study using a conditional knock-out strategy to investigate TH signalling in the hippocampal lineage. The importance of this approach is highlighted by a comparison with a global MCT8ko mouse model. The critical role of MCT8 in transporting T3 and T4 across brain barriers (Bernal et al., 2015; Ceballos et al., 2009; Trajkovic et al., 2007) means that the brain of global MCT8ko mice is in a mild hypothyroid state, affecting TH metabolism and regulation of TH target genes. That this causes non-cell

autonomous effects on neurogenesis is shown by our finding that at 6 months of age the number of NBs was not altered in MCT8-NSCko mice while it was increased in global MCT8ko mice. This increase cannot simply be explained by a hypothyroid neurogenic niche due to a global loss of MCT8. Both TRα1 mutant mice that show features of a hypothyroid CNS and globally hypothyroid animals exhibit a reduced number of DCX+ cells in the SGZ (Kapoor et al., 2010; Montero-Pedrazuela et al., 2006) while a rise in NB numbers was reported in TRα1ko, hyperthyroid TRβko or T3-treated mice (Kapoor et al., 2012; Kapoor et al., 2011; Kapoor et al., 2010). In the latter model, increased BrdU-labelling of DCX+ cells was attributed to earlier acquisition of DCX immunoreactivity (Kapoor et al., 2012). The increased EdU labelling in DCX+ cells we observe in MCT8ko animals may be explained in the same way, linked to the hyperthyroid periphery of MCT8ko mice (Trajkovic et al., 2007). In keeping with this, we do not see earlier DCX expression in slices treated with a MCT8 inhibitor, where the level of TH in the culture medium is normal. However, alterations in cell cycle entry or kinetics cannot be fully excluded.

Non-cell autonomous effects earlier in the lineage may also explain the differences observed in NSC and NB numbers at 2 and 6 months between MCT8ko and Wt animals. Reduced NSC activation in the global ko at 2 months (which as it is not seen in the MCT8-NSCko mice must be a non-cell autonomous effect of TH signalling) would be expected to preserve the NSC population and so explain the increased NSCs present in the MCT8ko at 6 months as compared to Wt mice at the same age. This in turn could attenuate the normal age-related decline in NBs (as would the earlier DCX expression discussed above), so explaining the smaller reduction in NBs at 6 months in these mice. Clearly, any of the neighbouring glial and vascular cell types could contribute to this non-cell autonomous effect. We hypothesise, however, that MCT8 deficient astrocytes contribute significantly through the previously described effects on TH-regulated components of the NOTCH or WNT signalling pathways (Morte et al., 2018).

The role of MCT8 at the differentiation stage of neurogenesis is of particular relevance to the pathophysiology of Allan-Herndon-Dudley syndrome (AHDS), a severe form of

313 psychomotor retardation caused by inactivating mutations in MCT8 (Dumitrescu et al., 2004;
314 Friesema et al., 2004; Schwartz et al., 2005). AHDS-like symptoms could be replicated only
315 by simultaneous inactivation of MCT8 and another TH transporter, OATP1C1, in mice (Mayerl
316 et al., 2014), from which we presumed that impaired TH transport across the BBB and/or
317 BCSFB is the major abnormality driving the disease phenotype. Our results that MCT8 loss
318 results in cell autonomous effects in NBs, however, suggests that a direct effect on the
319 formation of newly-born GCNs may also contribute to the phenotype.

320 MCT8 has recently been implicated in corticogenesis in the chicken optic tectum
321 (Vancamp et al., 2017), where knock-down resulted in a reduced progenitor pool and
322 diminished neurogenesis. Though we also observed reduced neurogenesis we found, in
323 contrast to Vancamp et al., that MCT8 was critical for later stages of the adult hippocampal
324 program in the mouse, i.e. the differentiation step from NBs to INs, and not for the regulation
325 of progenitor proliferation and pool size. This emphasizes that the mechanisms by which TH
326 signalling influences neurogenic processes vary between niches. Similarly, a different function
327 of the TH signal is documented in a third niche, the adult SVZ, where in contrast to the SGZ
328 T3/TRα1 signalling is involved in repressing NSC pluripotency and determining the progenitor
329 pool size (Remaud et al., 2014).

330 The organotypic hippocampal slice culture system that we established is likely to have
331 significant utility. Our protocol that allows adult slices to be maintained for up to 3 weeks
332 enables examination of all stages of adult neurogenesis and cell-fate monitoring of EdU+ cells.
333 We used the technique to show that application of the MCT8-specific inhibitor Silychristin
334 compromised generation of EdU+/NEUN+ neurons after 3 weeks in culture without effects on
335 EdU incorporation at earlier stages. This is in line with earlier in vivo studies of hypothyroid
336 rodents that reported either no effect or only a slightly reduced progenitor proliferation of in the
337 SGZ whereas formation of new neurons was impaired (Ambrogini et al., 2005; Desouza et al.,
338 2005; Montero-Pedrazuela et al., 2006). In comparison, application of the LAT-inhibitor BCH
339 or the deiodinase inhibitor iopanoic acid did not alter neurogenesis in hippocampal slices.

These findings underscore a prominent gate-keeper role of MCT8 in NBs and substantiate the view that in the SGZ TH predominantly acts on post-mitotic progenitors (Remaud et al., 2014).

To define a mechanism by which MCT8 in NBs is required for proper differentiation we investigated the expression of cell cycle/CDK inhibitors P21CIP1, P27KIP1 and P57KIP2. In line with recent work (Horster et al., 2017) we found pronounced P27 expression in SGZ NBs and INs of Wt mice whereas significantly lower P27 protein and mRNA levels were detected in MCT8ko and MCT8-NSCko mice. Based on that and reports showing *p27* as a TH-target gene (Garcia-Silva et al., 2002; Holsberger et al., 2003), we speculate that absence of MCT8 in NBs causes TH deficiency within the cells which in turn reduces the expression of P27 and inhibits differentiation. Consistent with this, P27 deficient mice have more proliferating cells in the SGZ, reduced levels of neurogenesis and specific cognitive impairments (Horster et al., 2017).

Our demonstration that in the CNS loss of MCT8 causes both cell autonomous and non-cell autonomous effects on neurogenesis will inform potential treatment strategies for AHDS where, in addition to any transport impairments across the BBB, effects of MCT8 loss in CNS cell populations will need to be addressed. Our findings also have important implications for therapeutic approaches addressing cognitive decline resulting from compromised hippocampal neurogenesis, where selective targeting of the cell autonomous functions of TH signalling may allow enhanced neuronal differentiation without the systemic effects of increased TH action.

Experimental Procedures

Animals

MCT8ko mice obtained from Deltagen were generated, bred and genotyped as described previously (Trajkovic et al., 2007). *Mct8*fl mice obtained from the KOMP repository (*Slc16a2*$^{tm1a(KOMP)Wtsi}$) were generated and genotyped as reported before (Mayerl et al., 2018). *Mct8* +/ko and *Mct8* +/fl females were bred with males (C57BL/6) carrying a Tamoxifen-inducible Cre recombinase driven by the *Nestin* promoter (Lagace et al., 2007) and a *Cre* reporter allele consisting of a loxP-flanked STOP cassette preventing transcription of a CAG promotor driven *tdTomato* construct (Madisen et al., 2010) purchased from Jackson laboratories (*C57BL/6-Tg[Nes-cre/ERT2]KEisc/J*, Jax stock #016261 and *B6.Cg-Gt(ROSA)26Sor*$^{tm9(CAG-tdTomato)Hze}$, Jax stock #007909). *Cre* and *tdTomato* (hereafter *Rfp*) transgenes were detected as described (Lagace et al., 2007; Madisen et al., 2010). At the age of 4-5 weeks, tamoxifen (180 mg/kg; Sigma-Aldrich) was administered to *Mct8* +/y, *Mct8* ko/y and *Mct8* fl/y male mice (note that the *Mct8* gene is located on the X-chromosome) harbouring both transgenes by oral gavage for 5 consecutive days and animals were kept for 5 months. For EdU labelling studies, mice (aged 2 or 6 months) were injected i.p. with 100 µl EdU (10 mg/ml; Thermo Fisher) in PBS 3 d or 28 d before sacrifice. 6-8 week old mice for hippocampal slice cultures were injected twice with EdU as above 4 h and 2 h before sacrifice.

Mice were kept at constant temperature (22 C) on a 12 h light, 12 h dark cycle and provided with standard chow and water *ad libitum*. Animals used for FACS studies were sacrificed by cervical dislocation at 2 months of age. For immunofluorescence studies mice were transcardially perfused with 4% PFA. Brains were cryo-protected with 30% sucrose, snap frozen in isopentane on dry ice and kept at -80 C. Mice designated for hippocampal slice culture were exposed to rising concentrations of CO_2 and brains were isolated rapidly. For all studies, male mice have been used.

FACS

For one run, brains of 8 C57BL/6N Wt mice were isolated, stored in chilled Hibernate A (Thermo Fisher) and dentate gyri were micro-dissected (Babu et al., 2011). Tissue was pooled and processed as described (Guez-Barber et al., 2012) and as summarised in the supplementary material.

Before fixation, cells were re-suspended in Hibernate A, incubated for 15 min with a fixable live/dead cell stain (LIVE/DEAD® Fixable Violet Dead Cell Stain Kit; 1:000; Life Technologies) at 4 C and pelleted by centrifugation at 4000 rpm for 4 min. For fixation, cells were re-suspended in 1 ml chilled Hibernate A, 3 ml of ice-cold 100% Ethanol (molecular grade; Sigma-Aldrich) was added, and cells were fixed in this 75% Ethanol solution at 4 C for 20 min (Diez et al., 1999). To increase mRNA yield and quality, all solutions used after this step were treated overnight with 1:1000 diethyl pyrocarbonate (Sigma-Aldrich) (Diez et al., 1999). After fixation, cells were pelleted as above and washed in 1 ml chilled PBS containing 0.1% saponin (Sigma-Aldrich), 0.2% BSA (Sigma-Aldrich) and 1:100 RNase inhibitor (RNaseOUT; Life Technologies) (Hrvatin et al., 2014). Staining procedures are detailed in the supplementary material.

Hippocampal neurogenic populations were sorted with a FACS Aria II (BD Bioscience) into chilled RNase-free tubes containing 100 µl FACS buffer. All marker-negative cells were collected separately for RNA quality determination. If the final volume per tube exceeded 300 µl, cells were pelleted by centrifugation for 10 min at 13200 rpm and 4 C. Cells were frozen on dry ice and stored at -80 C.

Adult hippocampal slice culture

Mouse brains were isolated and transferred into chilled dissection buffer (Hibernate A with 2% B27 supplement (Life Technologies), 2 mM L-Glutamine and 1% Penicillin/Streptomycin) on ice as described (Kim et al., 2013). Tissue was sectioned as published previously (Kleine Borgmann et al., 2013) in chilled dissection buffer using a vibratome. 300 µm sections were stored in dissection buffer on ice and transferred onto Millicell inserts (Millipore). Organotypic slices were cultured at 37 C and 5% CO_2 in a serum-free

medium (Kim et al., 2013) (Neurobasal A (Life Technologies) containing 2% B27 supplement, 2 mM L-Glutamine, 1% Penicillin/Streptomycin and 80 µM Indomethacin (Sigma-Aldrich)). During the entire culture period slices were exposed to 25 µM Silychristin (Sigma-Aldrich), 10 µM iopanoic acid (Sigma-Aldrich), 1 mM BCH (R&D systems) or respective volumes of the solvents DMSO or culture medium as control. Culture medium was replaced every other day and slices were fixed for 1 h in 4% PFA.

Immunofluorescence studies, Quantification and RT-PCR

Procedures are described in the supplementary material.

qPCR

Total RNA from FACsorted hippocampal populations and respective controls was isolated using the RNEasy Micro Kit (Qiagen). RNA quality was assessed in controls on a high sensitivity screen tape (Agilent Technologies). At least 100.000 cells from control sorts were subjected to RIN value assessment. Samples were only processed further if RIN≥7. Two rounds of RNA amplification were conducted using the ExpressArt C&E PICO RNA Amplification kit (AMS Biotechnology) following the manufacturer's instructions. RNA concentration was analysed with a RNA screentape (Agilent Technologies). If necessary, a third round of RNA amplification was performed and quantity was measured as before. 250 ng of RNA were subjected to cDNA synthesis using the SuperScript First-Strand Synthesis System (Invitrogen). Quantitative Real-Time PCR (qPCR) was performed using the QuantiFast SYBR Green PCR Kit (Qiagen) and the LightCycler® 480 system (Roche). Further information can be found in the supplementary material.

Statistics

All data represent mean+SEM. In slice culture experiments, to compare Wt vs. MCT8ko animals and control vs. MCT8-NSCko mice statistical significance between groups was

443 determined by unpaired two-tailed Student's *t* test. Differences were considered significant
444 when $P < 0.05$ and marked as follows: *, $P < 0.05$; **, $P < 0.01$; ***, $P < 0.001$.
445
446 *Study approval*
447 All studies were executed in compliance with UK Home Office regulations and local
448 guidelines by The University of Edinburgh.

Acknowledgments:

This work was supported by grants of the DFG to SM (MA7212/2-1) and HH (HE3418/8-1 within the SPP1629). We thank SCRM animal facility staff (Luke McPhee, Chris Wilson, Lorraine McNeil, John Agnew and Jamie Kelly) for their excellent help. We are also grateful to Fiona Rossi and Claire Cryer (SCRM FACS facility) and Bertrand Vernay (SCRM imaging facility) for support.

Author contributions:

SM devised, conducted, and analysed the experiments. SM and CffC interpreted the results. HH provided *Mct8*ko and *Mct8*fl mice as well as valuable expertise on TH signalling. SM, HH and CffC wrote the manuscript.

Disclosure Statement:

The authors have nothing to disclose.

References:

Ambrogini, P., Cuppini, R., Ferri, P., Mancini, C., Ciaroni, S., Voci, A., Gerdoni, E., and Gallo, G. (2005). Thyroid hormones affect neurogenesis in the dentate gyrus of adult rat. Neuroendocrinology *81*, 244-253.

Astapova, I., and Hollenberg, A.N. (2013). The in vivo role of nuclear receptor corepressors in thyroid hormone action. Biochim Biophys Acta *1830*, 3876-3881.

Babu, H., Claasen, J.H., Kannan, S., Rünker, A.E., Palmer, T., and Kempermann, G. (2011). A protocol for isolation and enriched monolayer cultivation of neural precursor cells from mouse dentate gyrus. Front Neurosci *5*, 89.

Beckervordersandforth, R., Zhang, C.L., and Lie, D.C. (2015). Transcription-Factor-Dependent Control of Adult Hippocampal Neurogenesis. Cold Spring Harb Perspect Biol *7*, a018879.

Ben Abdallah, N.M., Slomianka, L., Vyssotski, A.L., and Lipp, H.P. (2010). Early age-related changes in adult hippocampal neurogenesis in C57 mice. Neurobiol Aging *31*, 151-161.

Bernal, J., Guadano-Ferraz, A., and Morte, B. (2015). Thyroid hormone transporters--functions and clinical implications. Nat Rev Endocrinol *11*, 406-417.

Bianco, A.C., Salvatore, D., Gereben, B., Berry, M.J., and Larsen, P.R. (2002). Biochemistry, cellular and molecular biology, and physiological roles of the iodothyronine selenodeiodinases. Endocr Rev *23*, 38-89.

Ceballos, A., Belinchon, M.M., Sanchez-Mendoza, E., Grijota-Martinez, C., Dumitrescu, A.M., Refetoff, S., Morte, B., and Bernal, J. (2009). Importance of monocarboxylate transporter 8 for the blood-brain barrier-dependent availability of 3,5,3'-triiodo-L-thyronine. Endocrinology *150*, 2491-2496.

Cooke, G.E., Mullally, S., Correia, N., O'Mara, S.M., and Gibney, J. (2014). Hippocampal volume is decreased in adults with hypothyroidism. Thyroid *24*, 433-440.

Correia, N., Mullally, S., Cooke, G., Tun, T.K., Phelan, N., Feeney, J., Fitzgibbon, M., Boran, G., O'Mara, S., and Gibney, J. (2009). Evidence for a specific defect in hippocampal memory in overt and subclinical hypothyroidism. J Clin Endocrinol Metab *94*, 3789-3797.

Dentice, M., Marsili, A., Zavacki, A., Larsen, P.R., and Salvatore, D. (2013). The deiodinases and the control of intracellular thyroid hormone signaling during cellular differentiation. Biochim Biophys Acta *1830*, 3937-3945.

Desouza, L.A., Ladiwala, U., Daniel, S.M., Agashe, S., Vaidya, R.A., and Vaidya, V.A. (2005). Thyroid hormone regulates hippocampal neurogenesis in the adult rat brain. Mol Cell Neurosci *29*, 414-426.

Diez, C., Bertsch, G., and Simm, A. (1999). Isolation of full-size mRNA from cells sorted by flow cytometry. J Biochem Biophys Methods *40*, 69-80.

Dumitrescu, A.M., Liao, X.H., Best, T.B., Brockmann, K., and Refetoff, S. (2004). A novel syndrome combining thyroid and neurological abnormalities is associated with mutations in a monocarboxylate transporter gene. Am J Hum Genet *74*, 168-175.

Flamant, F., and Gauthier, K. (2013). Thyroid hormone receptors: the challenge of elucidating isotype-specific functions and cell-specific response. Biochim Biophys Acta *1830*, 3900-3907.

Friesema, E.C., Grueters, A., Biebermann, H., Krude, H., von Moers, A., Reeser, M., Barrett, T.G., Mancilla, E.E., Svensson, J., Kester, M.H.*, et al.* (2004). Association between mutations in a thyroid hormone transporter and severe X-linked psychomotor retardation. Lancet *364*, 1435-1437.

Garcia-Silva, S., Perez-Juste, G., and Aranda, A. (2002). Cell cycle control by the thyroid hormone in neuroblastoma cells. Toxicology *181-182*, 179-182.

Gerlach, J., Donkels, C., Münzner, G., and Haas, C.A. (2016). Persistent Gliosis Interferes with Neurogenesis in Organotypic Hippocampal Slice Cultures. Front Cell Neurosci *10*, 131.

Guez-Barber, D., Fanous, S., Harvey, B.K., Zhang, Y., Lehrmann, E., Becker, K.G., Picciotto, M.R., and Hope, B.T. (2012). FACS purification of immunolabeled cell types from adult rat brain. J Neurosci Methods *203*, 10-18.

Heuer, H., and Visser, T.J. (2013). The pathophysiological consequences of thyroid hormone transporter deficiencies: Insights from mouse models. Biochim Biophys Acta *1830*, 3974-3978.
Holsberger, D.R., Jirawatnotai, S., Kiyokawa, H., and Cooke, P.S. (2003). Thyroid hormone regulates the cell cycle inhibitor p27Kip1 in postnatal murine Sertoli cells. Endocrinology *144*, 3732-3738.
Horster, H., Garthe, A., Walker, T.L., Ichwan, M., Steiner, B., Khan, M.A., Lie, D.C., Nicola, Z., Ramirez-Rodriguez, G., and Kempermann, G. (2017). p27kip1 Is Required for Functionally Relevant Adult Hippocampal Neurogenesis in Mice. Stem Cells *35*, 787-799.
Hrvatin, S., Deng, F., O'Donnell, C.W., Gifford, D.K., and Melton, D.A. (2014). MARIS: method for analyzing RNA following intracellular sorting. PLoS One *9*, e89459.
Ittermann, T., Wittfeld, K., Nauck, M., Bulow, R., Hosten, N., Volzke, H., and Grabe, H.J. (2018). High Thyrotropin Is Associated with Reduced Hippocampal Volume in a Population-Based Study from Germany. Thyroid *28*, 1434-1442.
Johannes, J., Jayarama-Naidu, R., Meyer, F., Wirth, E.K., Schweizer, U., Schomburg, L., Kohrle, J., and Renko, K. (2016). Silychristin, a Flavonolignan Derived From the Milk Thistle, Is a Potent Inhibitor of the Thyroid Hormone Transporter MCT8. Endocrinology *157*, 1694-1701.
Kapoor, R., Desouza, L.A., Nanavaty, I.N., Kernie, S.G., and Vaidya, V.A. (2012). Thyroid hormone accelerates the differentiation of adult hippocampal progenitors. J Neuroendocrinol *24*, 1259-1271.
Kapoor, R., Ghosh, H., Nordstrom, K., Vennstrom, B., and Vaidya, V.A. (2011). Loss of thyroid hormone receptor beta is associated with increased progenitor proliferation and NeuroD positive cell number in the adult hippocampus. Neurosci Lett *487*, 199-203.
Kapoor, R., van Hogerlinden, M., Wallis, K., Ghosh, H., Nordstrom, K., Vennstrom, B., and Vaidya, V.A. (2010). Unliganded thyroid hormone receptor alpha1 impairs adult hippocampal neurogenesis. FASEB J *24*, 4793-4805.
Kempermann, G., Jessberger, S., Steiner, B., and Kronenberg, G. (2004). Milestones of neuronal development in the adult hippocampus. Trends Neurosci *27*, 447-452.
Kim, H., Kim, E., Park, M., Lee, E., and Namkoong, K. (2013). Organotypic hippocampal slice culture from the adult mouse brain: a versatile tool for translational neuropsychopharmacology. Prog Neuropsychopharmacol Biol Psychiatry *41*, 36-43.
Kleine Borgmann, F.B., Bracko, O., and Jessberger, S. (2013). Imaging neurite development of adult-born granule cells. Development *140*, 2823-2827.
Koenig, R.J., Lazar, M.A., Hodin, R.A., Brent, G.A., Larsen, P.R., Chin, W.W., and Moore, D.D. (1989). Inhibition of thyroid hormone action by a non-hormone binding c-erbA protein generated by alternative mRNA splicing. Nature *337*, 659-661.
Kuhn, H.G., Toda, T., and Gage, F.H. (2018). Adult Hippocampal Neurogenesis: A Coming-of-Age Story. J Neurosci *38*, 10401-10410.
Lagace, D.C., Whitman, M.C., Noonan, M.A., Ables, J.L., DeCarolis, N.A., Arguello, A.A., Donovan, M.H., Fischer, S.J., Farnbauch, L.A., Beech, R.D.*, et al.* (2007). Dynamic contribution of nestin-expressing stem cells to adult neurogenesis. J Neurosci *27*, 12623-12629.
Madisen, L., Zwingman, T.A., Sunkin, S.M., Oh, S.W., Zariwala, H.A., Gu, H., Ng, L.L., Palmiter, R.D., Hawrylycz, M.J., Jones, A.R.*, et al.* (2010). A robust and high-throughput Cre reporting and characterization system for the whole mouse brain. Nat Neurosci *13*, 133-140.
Mayerl, S., Muller, J., Bauer, R., Richert, S., Kassmann, C.M., Darras, V.M., Buder, K., Boelen, A., Visser, T.J., and Heuer, H. (2014). Transporters MCT8 and OATP1C1 maintain murine brain thyroid hormone homeostasis. J Clin Invest *124*, 1987-1999.
Mayerl, S., Schmidt, M., Doycheva, D., Darras, V.M., Huttner, S.S., Boelen, A., Visser, T.J., Kaether, C., Heuer, H., and von Maltzahn, J. (2018). Thyroid Hormone Transporters MCT8 and OATP1C1 Control Skeletal Muscle Regeneration. Stem Cell Reports *10*, 1959-1974.
Melo-Salas, M.S., Perez-Dominguez, M., and Zepeda, A. (2018). Systemic Inflammation Impairs Proliferation of Hippocampal Type 2 Intermediate Precursor Cells. Cell Mol Neurobiol *38*, 1517-1528.

Miller, K.J., Parsons, T.D., Whybrow, P.C., van Herle, K., Rasgon, N., van Herle, A., Martinez, D., Silverman, D.H., and Bauer, M. (2006). Memory improvement with treatment of hypothyroidism. Int J Neurosci *116*, 895-906.
Montero-Pedrazuela, A., Venero, C., Lavado-Autric, R., Fernandez-Lamo, I., Garcia-Verdugo, J.M., Bernal, J., and Guadano-Ferraz, A. (2006). Modulation of adult hippocampal neurogenesis by thyroid hormones: implications in depressive-like behavior. Mol Psychiatry *11*, 361-371.
Morte, B., Gil-Ibanez, P., and Bernal, J. (2018). Regulation of Gene Expression by Thyroid Hormone in Primary Astrocytes: Factors Influencing the Genomic Response. Endocrinology *159*, 2083-2092.
Osterweil, D., Syndulko, K., Cohen, S.N., Pettler-Jennings, P.D., Hershman, J.M., Cummings, J.L., Tourtellotte, W.W., and Solomon, D.H. (1992). Cognitive function in non-demented older adults with hypothyroidism. J Am Geriatr Soc *40*, 325-335.
Remaud, S., Gothie, J.D., Morvan-Dubois, G., and Demeneix, B.A. (2014). Thyroid hormone signaling and adult neurogenesis in mammals. Front Endocrinol (Lausanne) *5*, 62.
Ritchie, J.W., Peter, G.J., Shi, Y.B., and Taylor, P.M. (1999). Thyroid hormone transport by 4F2hc-IU12 heterodimers expressed in Xenopus oocytes. J Endocrinol *163*, R5-9.
Ritchie, J.W., Shi, Y.B., Hayashi, Y., Baird, F.E., Muchekehu, R.W., Christie, G.R., and Taylor, P.M. (2003). A role for thyroid hormone transporters in transcriptional regulation by thyroid hormone receptors. Mol Endocrinol *17*, 653-661.
Schwartz, C.E., May, M.M., Carpenter, N.J., Rogers, R.C., Martin, J., Bialer, M.G., Ward, J., Sanabria, J., Marsa, S., Lewis, J.A.*, et al.* (2005). Allan-Herndon-Dudley syndrome and the monocarboxylate transporter 8 (MCT8) gene. Am J Hum Genet *77*, 41-53.
Suzuki, S., Mori, J., and Hashizume, K. (2007). mu-crystallin, a NADPH-dependent T(3)-binding protein in cytosol. Trends Endocrinol Metab *18*, 286-289.
Trajkovic, M., Visser, T.J., Mittag, J., Horn, S., Lukas, J., Darras, V.M., Raivich, G., Bauer, K., and Heuer, H. (2007). Abnormal thyroid hormone metabolism in mice lacking the monocarboxylate transporter 8. J Clin Invest *117*, 627-635.
Vancamp, P., Deprez, M.A., Remmerie, M., and Darras, V.M. (2017). Deficiency of the Thyroid Hormone Transporter Monocarboxylate Transporter 8 in Neural Progenitors Impairs Cellular Processes Crucial for Early Corticogenesis. J Neurosci *37*, 11616-11631.

Fig.1: Alterations in mRNA expression of TH signalling components during adult hippocampal neurogenesis.

Micro-dissected dentate gyri were subjected to FACS and neurogenic/neuronal populations were sorted according to their expression of intracellular markers. A) Schematic representation of the hippocampal neurogenic program illustrating expression of stage-specific markers used for sorting and validation strategies. B) qPCR analysis of neurogenic markers showing that isolated populations are of the expected identity. Relative mRNA expression of (C) TH transporters, (D) TH receptor isoforms, and (E) accessory proteins are depicted. Transcript levels were normalised to *Gapdh* expression and transcript expression in GCN. Note that due to their absence from GCN samples, *Hes5* and *Lat1* values were normalised to NSC levels while *Dcx* expression was normalised to NB values. n=2-4 individual samples per cell population.

Fig.2: Spatiotemporal protein expression of TH signalling components.

A) Perfusion-fixed coronal forebrain cryosections were immunostained to visualize DIO3, LAT1, LAT2, MCT8, and MCT10 protein (green) in the SGZ in GFAP+ (magenta)/SOX2+ (blue) NSCs, in MCM2+ (magenta) proliferating cells, in DCX+ (magenta) cells either negative for CR (type 2b progenitors and NBs) or CR+ (blue; INs), and in CB+ (magenta) GCNs. Nuclei were stained with Hoechst33258 (grey). B) MCT8 (green) co-stained with MCM2 (blue) in DCX+ (magenta; arrowhead) but not DCX- (*) cells. Cell nuclei counterstained by Hoechst33258 are displayed in grey. C) Distribution of DIO3, LAT2, MCT8, and MCT10 (green) over the height of the suprapyramidal blade of the dentate gyrus. Nuclei were stained for Hoechst33258 (grey) and mature GCNs were identified by CB (magenta). DIO3 and LAT2 protein are asymmetrically distributed with higher signal intensities in areas close to the molecular layer while MCT8 and MCT0 appear evenly dispersed.

Fig.3: Inhibition of MCT8 in adult slices perturbs neuron formation.

After acute EdU injection, adult brain slices cultured ex vivo for up to 3 weeks. Lineage progression in the presence of TH signalling inhibitors was assessed. A) Exemplar pictures from adult slices grown in control medium. EdU incorporation (magenta) into proliferating cells (KI67+, green) was visualised after 1 day; into DCX+ cells (type 2b progenitors, NBs and INs) after 7 days; and into newly formed neurons (NEUN positive, green) after 21 days. Hoechst33258-counterstained nuclei are shown in blue. Total number of EdU+ cells (B) and incorporation of EdU into KI67+ cells (C) after 1 day in culture, EdU+/DCX+ cells at Day7 (D) and newly formed neurons (EdU+/NEUN+) at Day21 (E) upon exposure to 25 µM Silychristin were quantified. n=4-6 mice per condition.

Fig.4: Adult hippocampal neurogenesis is altered in 2 months old MCT8ko mice.

Perfusion-fixed cryosections of 2-month-old Wt and MCT8ko littermates were immunostained for stage-specific markers of hippocampal neurogenesis. A) Total numbers of GFAP+(cyan) and SOX2+(yellow) NSCs (arrowheads) harbouring a single process protruding into the granule cell layer, and activated NSCs (KI67+; magenta; arrows). B) Overall numbers of proliferating cells in the SGZ (all KI67+ cells; green; arrowheads) and numbers of proliferating type 2b/NBs expressing KI67 and DCX (magenta; arrows). C) DCX(magenta) and CR(green) were used to discriminate between type 2b progenitors/NBs (only DCX+; arrows) and INs (DCX+/CR+, arrowheads). D) Timeline of EdU labelling experiments. Injected at P60, mice were perfused 3 d or 28 d later and stained as shown. E) EdU(cyan) retention in proliferating progenitors (KI67+; yellow; arrowheads) and DCX+ (magenta; arrows) cells was assessed at 3 dpi. F) Incorporation of EdU (cyan) into type 2b progenitors/NBs (DCX+ (magenta)/CR- (yellow); arrows) and into INs (DCX+/CR+; arrowheads). G) 28 days after EdU pulse, GCN formation (CB+(green) and EdU(magenta)) was analysed. In all experiments, cell nuclei were counter-stained with Hoechst33258 (blue). n=4 (28 dp EdU) or n=6 (3 dp EdU) mice per genotype.

Fig.5: MCT8 deficiency compromises adult hippocampal neurogenesis at 6 months of age.

Neurogenesis was assessed in 6-month-old males. A) Numbers of GFAP+ (cyan)/SOX2+ (yellow) NSCs with a radial process (arrowheads) as well as density of activated KI67+ (magenta, arrow) NSCs. B) Proliferation 3 d after EdU injection. Overall KI67+ (cyan; arrows) and KI67+/EdU+ (yellow) cell numbers are shown. Late stage proliferating cells expressing DCX (magenta, arrowheads) show a higher proliferative capacity. C) Density of DCX+ (magenta)/CR- (cyan) type 2b progenitors/NBs (arrowheads) as well as of DCX+/CR+ INs (arrows) with or without EdU (3 dpi; yellow). D) Newly formed GCNs (arrowheads) positive for CB (green) and EdU (magenta) were visualised 28 d after EdU injection. E) Breeding strategy to generate males harbouring the Wt or *Mct8*ko allele as well as *Nestin-CreERT2* and *Rfp* reporter transgenes. Animals were gavaged for 5 consecutive days at 4 weeks of age and perfused at 6 months of age. F) Numbers of GFAP+(cyan)/SOX2+(yellow) NSCs (arrows) with a radial process and of RFP+ (in magenta, arrowheads) NSCs were counted and quantified as per mm and % of RFP+ cells. G) RFP+ (magenta)/ CB+ (green) GCNs (arrowheads) were counted and normalised to the number of RFP+ cells. Cell nuclei were stained with Hoechst33258 (blue). n=4 (28 dp EdU and *Nestin-Cre; Rfp* animals) or n=6 (3 dp EdU injection) mice per genotype.

Fig.6: Absence of MCT8 in NSCs compromises adult hippocampal neurogenesis.

A) *Mct8*fl/+ females were bred with males carrying *Nestin-CreERT2* and *Rfp* reporter alleles to generate *Mct8*+/y, *Nestin-CreERT2*, *Rfp* (control) and *Mct8fl*/y, *Nestin-CreERT2*, *Rfp* (MCT8-NSCko) littermates. Tamoxifen was given for 5 consecutive days at 4 weeks of age and animals were perfused at 6 months of age. B) Number of RFP+ (magenta)/GFAP+ (yellow)/SOX2+ (cyan) NSCs per mm SGZ and their % contribution to all RFP+ cells were determined. C-F) Relative numbers of RFP+ (magenta; arrowheads)-labelled activated NSCs (KI67+(yellow)/GFAP+(cyan)) (C), proliferating cells (KI67+; cyan) and proliferating DCX+(yellow) cells (D), apoptotic cells (CASPASE3+; green) (E), DCX+(cyan)/CR-(yellow)

type 2b progenitors/NBs and RFP+/DCX+/CR+ INs (arrows) (F). (G) Ratio of RFP+ (magenta)/CB+ (green) GCNs (arrowheads) over all RFP+ cells. Hoechst33258 labelled cell nuclei are depicted in blue. n=5 mice per genotype.

Fig.7: Cell cycle inhibitor expression is altered in MCT8 deficiency.

A) Representative overview images and magnified views of P27KIP1(green) staining in DCX+ (magenta) type 2b progenitors/NBs and DCX+/CR+(blue) INs at 2 months of age. Normalised nuclear P27 fluorescent signal intensities were quantified. B) P27 immunoreactivity in type 2b progenitors/NBs and INs was measured at 6 months of age. C) Sections from 6-month-old MCT8-NSCko and control brains were stained for P27KIP1(green), DCX(blue) and CR(grey). RFP fluorescence is shown in magenta. Magnified views depict CR-/RFP+/DCX+ cells. Normalised P27 signal intensities were compared. D, E) P21(green) was analysed at 2 months (D) and 6 months of age (E). F, G) P57 (in green) fluorescence intensities were assessed at 2 months (F) and 6 months (G) of age. Hoechst33258 positive nuclei are shown in grey, DCX in magenta and CR in blue. n=6 (A, B, D-G) and n=4-5 (C) mice per genotype.

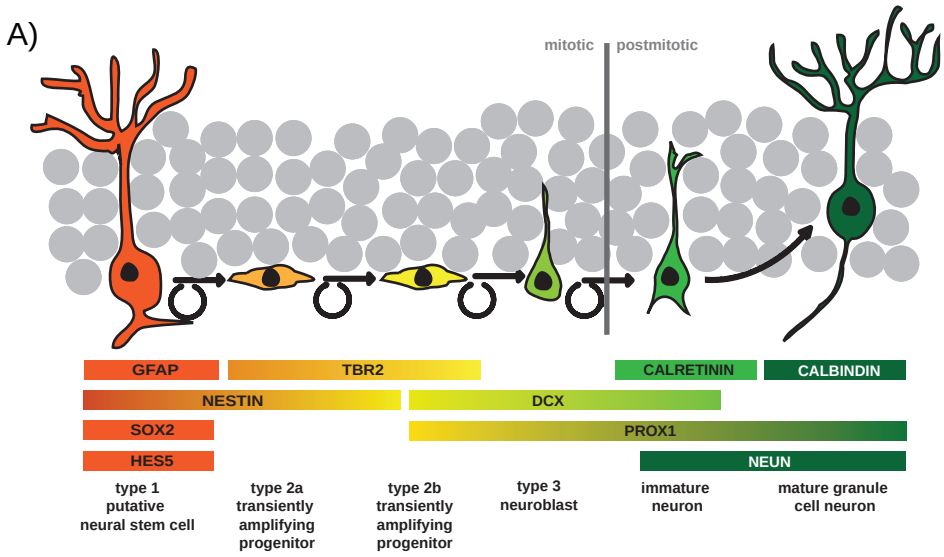
A)
mitotic
postmitotic
GFAP
TBR2
CALRETININ
CALBINDIN
NESTIN
DCX
SOX2
PROX1
HES5
NEUN
type 1 putative neural stem cell
type 2a transiently amplifying progenitor
type 2b transiently amplifying progenitor
type 3 neuroblast
immature neuron
mature granule cell neuron

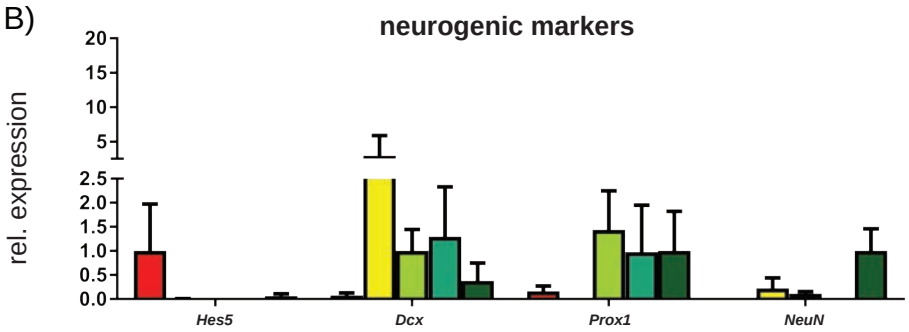
B)
neurogenic markers
rel. expression
20
15
10
5
2.5
2.0
1.5
1.0
0.5
0.0
Hes5
Dcx
Prox1
NeuN

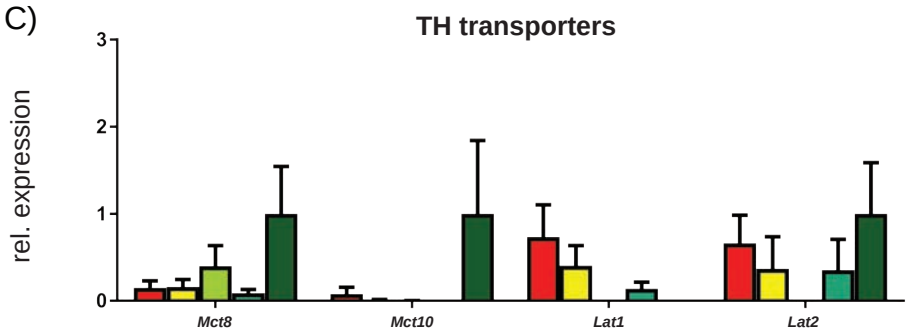
C)
TH transporters
rel. expression
3
2
1
0
Mct8
Mct10
Lat1
Lat2

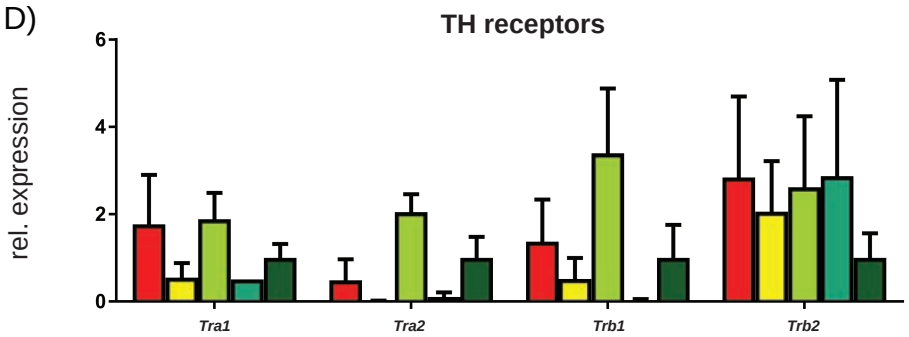
D)
TH receptors
rel. expression
6
4
2
0
Tra1
Tra2
Trb1
Trb2

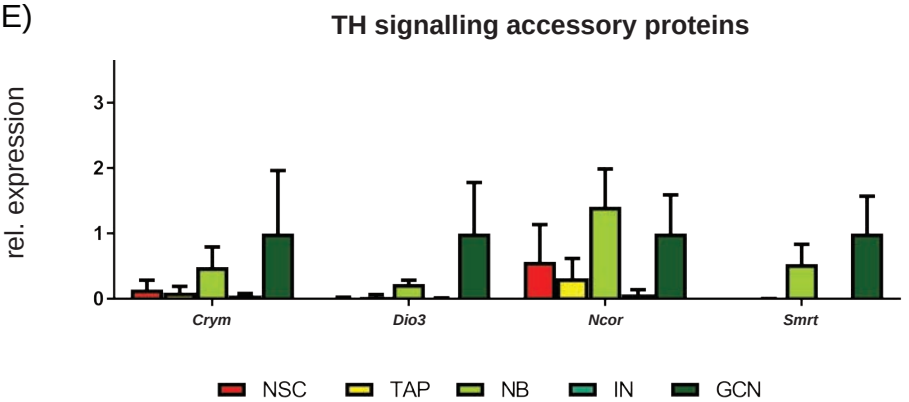
E)
TH signalling accessory proteins
rel. expression
3
2
1
0
Crym
Dio3
Ncor
Smrt
NSC
TAP
NB
IN
GCN

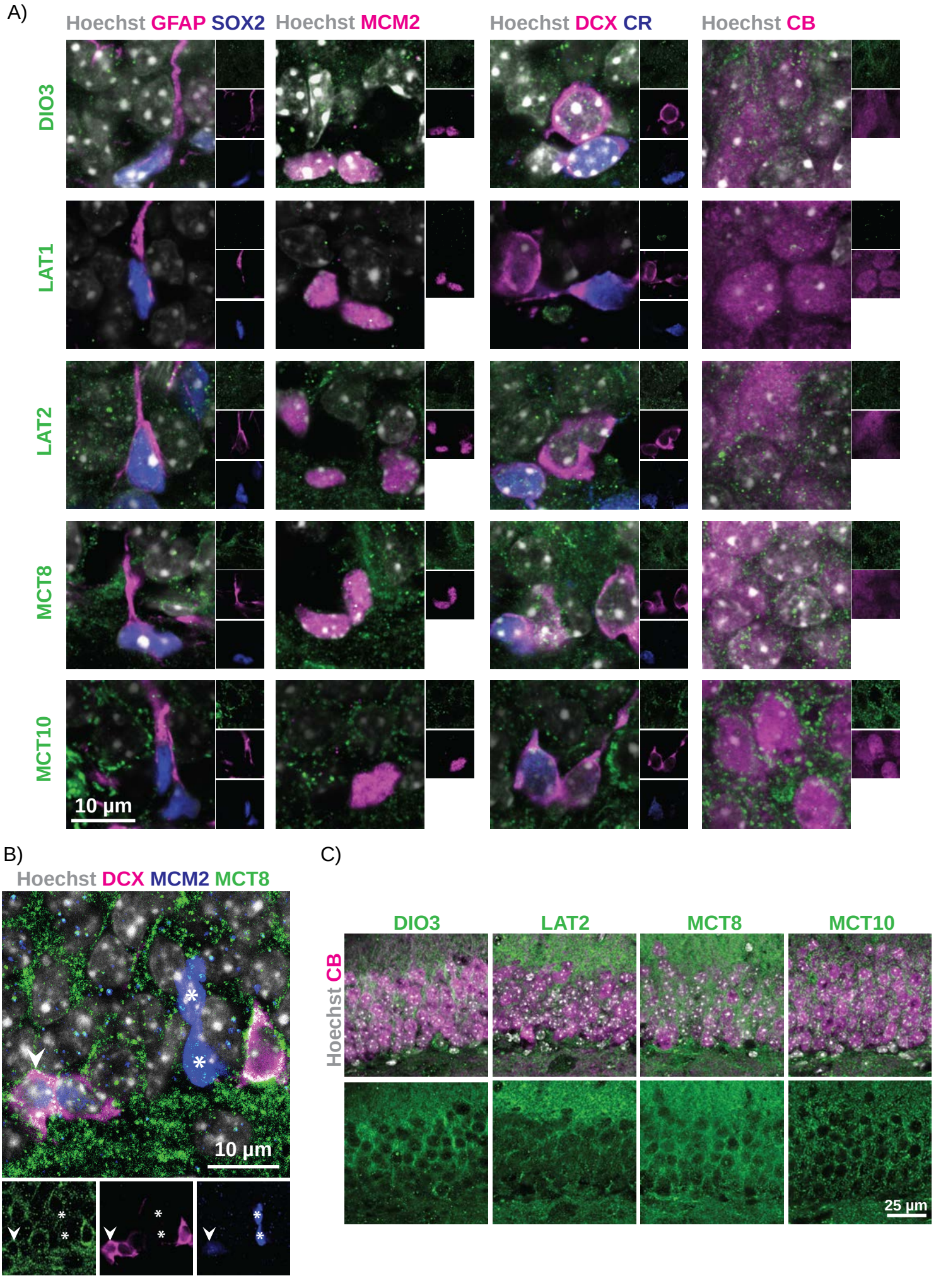
A)
Hoechst GFAP SOX2
Hoechst MCM2
Hoechst DCX CR
Hoechst CB
DIO3
LAT1
LAT2
MCT8
MCT10
10 µm
B)
Hoechst DCX MCM2 MCT8
10 µm
C)
DIO3
LAT2
MCT8
MCT10
Hoechst CB
25 µm

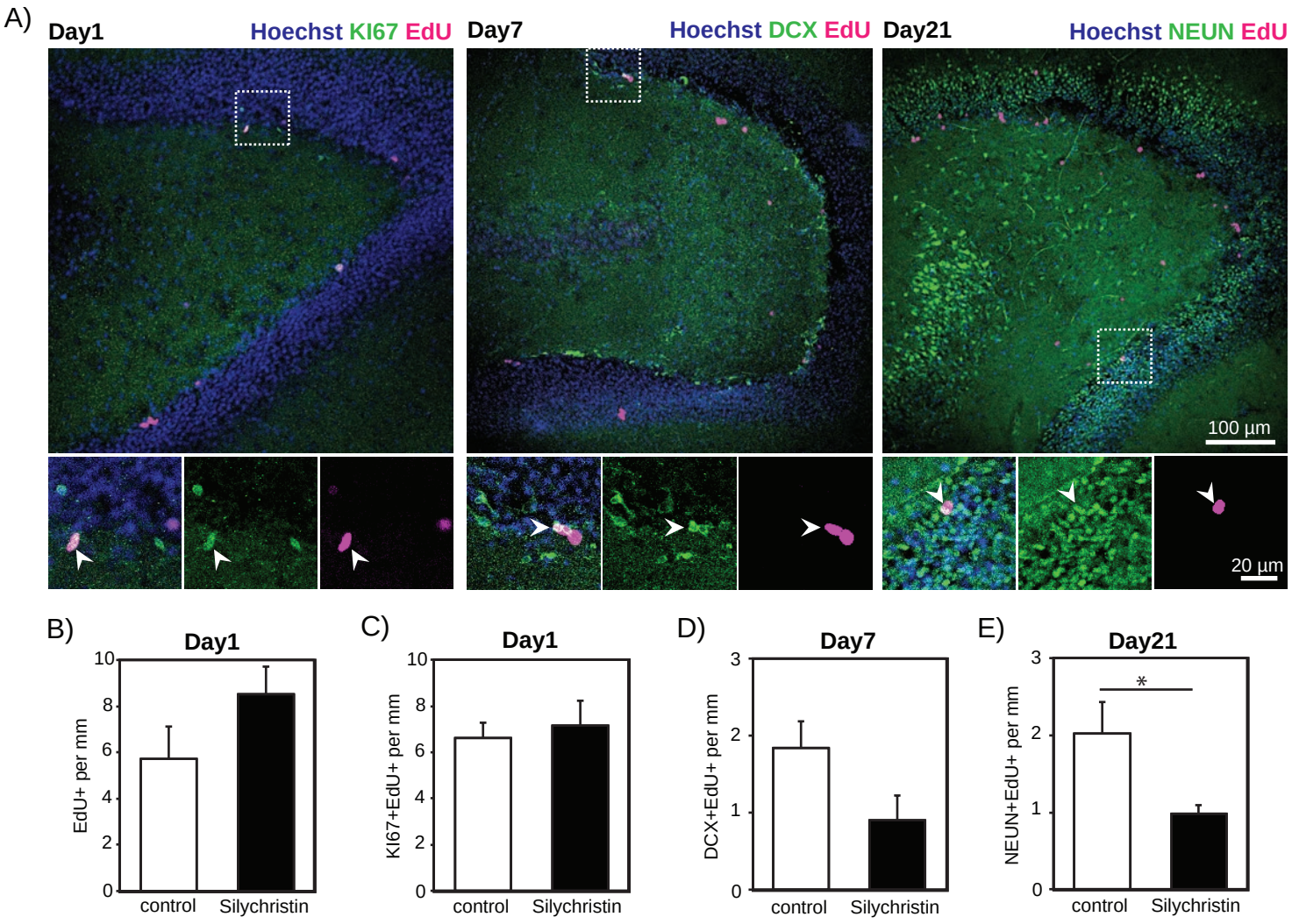
A)
Day1
Hoechst KI67 EdU
Day7
Hoechst DCX EdU
Day21
Hoechst NEUN EdU
100 µm
20 µm
B)
Day1
EdU+ per mm
control
Silychristin
C)
Day1
KI67+EdU+ per mm
control
Silychristin
D)
Day7
DCX+EdU+ per mm
control
Silychristin
E)
Day21
NEUN+EdU+ per mm
*
control
Silychristin

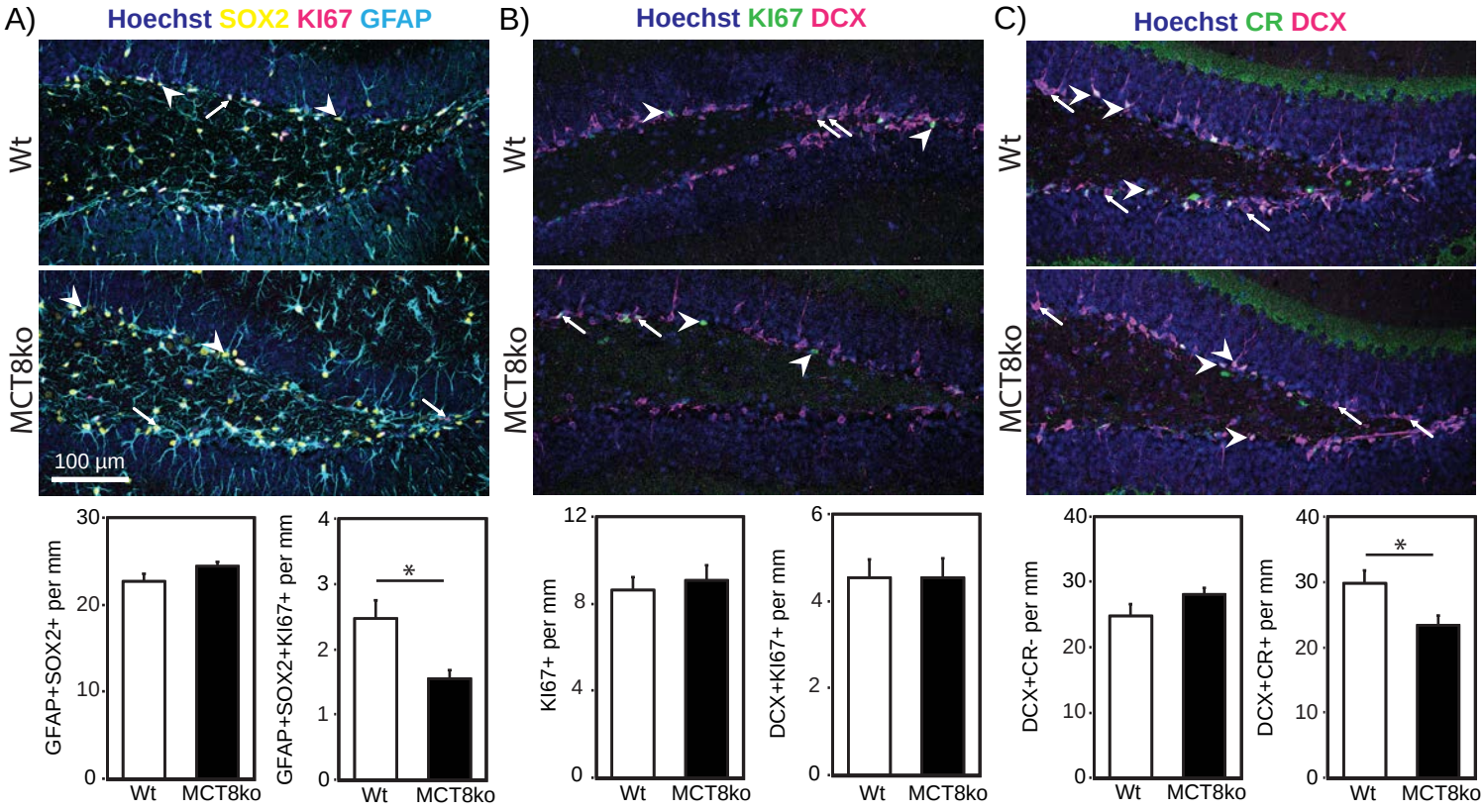
A)
Hoechst SOX2 KI67 GFAP
Wt
MCT8ko
100 µm
GFAP+SOX2+ per mm
GFAP+SOX2+KI67+ per mm
B)
Hoechst KI67 DCX
KI67+ per mm
DCX+KI67+ per mm
C)
Hoechst CR DCX
DCX+CR- per mm
DCX+CR+ per mm
Wt
MCT8ko
*

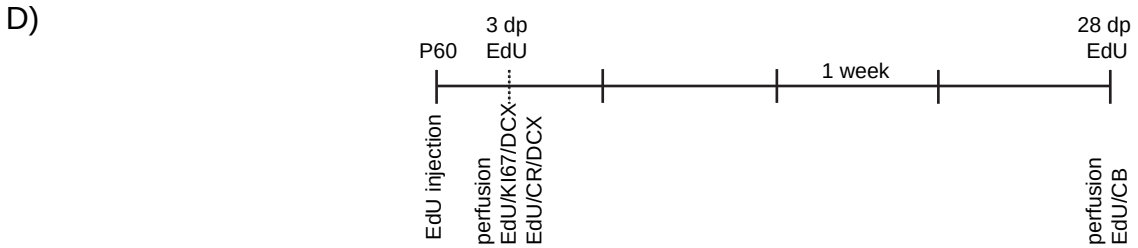
D)
P60
3 dp EdU
1 week
28 dp EdU
EdU injection
perfusion EdU/KI67/DCX EdU/CR/DCX
perfusion EdU/CB

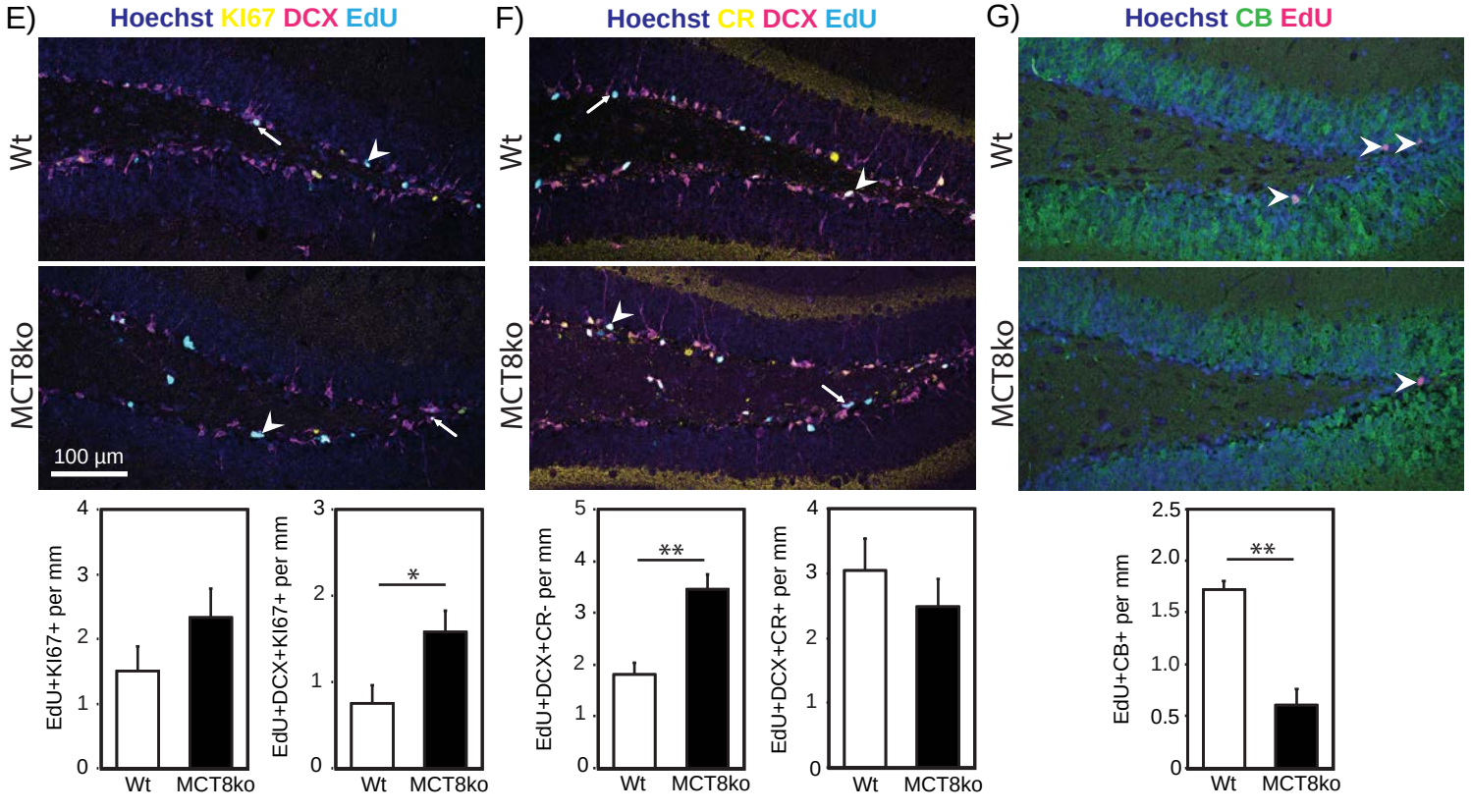
E)
Hoechst KI67 DCX EdU
Wt
MCT8ko
100 µm
EdU+KI67+ per mm
EdU+DCX+KI67+ per mm
F)
Hoechst CR DCX EdU
EdU+DCX+CR- per mm
EdU+DCX+CR+ per mm
G)
Hoechst CB EdU
EdU+CB+ per mm
Wt
MCT8ko
*
**

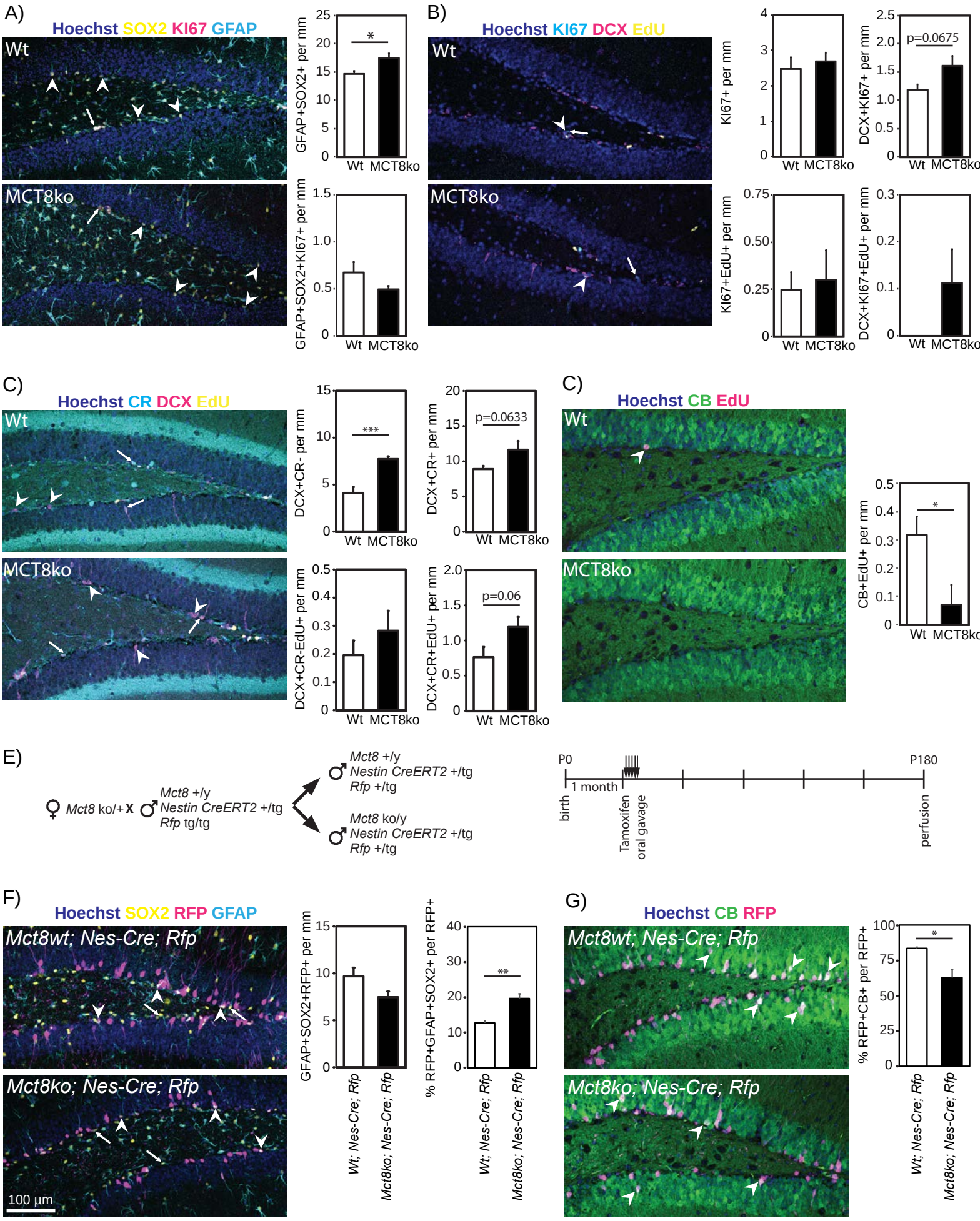
A)
Hoechst SOX2 KI67 GFAP
Wt
MCT8ko
GFAP+SOX2+ per mm
GFAP+SOX2+KI67+ per mm
B)
Hoechst KI67 DCX EdU
KI67+ per mm
DCX+KI67+ per mm
p=0.0675
KI67+EdU+ per mm
DCX+KI67+EdU+ per mm
C)
Hoechst CR DCX EdU
DCX+CR- per mm
DCX+CR+ per mm
p=0.0633
DCX+CR-EdU+ per mm
DCX+CR+EdU+ per mm
p=0.06
C)
Hoechst CB EdU
CB+EdU+ per mm
E)
♀ Mct8 ko/+ X ♂ Mct8 +/y Nestin CreERT2 +/tg Rfp tg/tg
♂ Mct8 +/y Nestin CreERT2 +/tg Rfp +/tg
♂ Mct8 ko/y Nestin CreERT2 +/tg Rfp +/tg
P0
P180
1 month
birth
Tamoxifen oral gavage
perfusion
F)
Hoechst SOX2 RFP GFAP
Mct8wt; Nes-Cre; Rfp
Mct8ko; Nes-Cre; Rfp
100 µm
GFAP+SOX2+RFP+ per mm
% RFP+GFAP+SOX2+ per RFP+
Wt; Nes-Cre; Rfp
Mct8ko; Nes-Cre; Rfp
G)
Hoechst CB RFP
% RFP+CB+ per RFP+

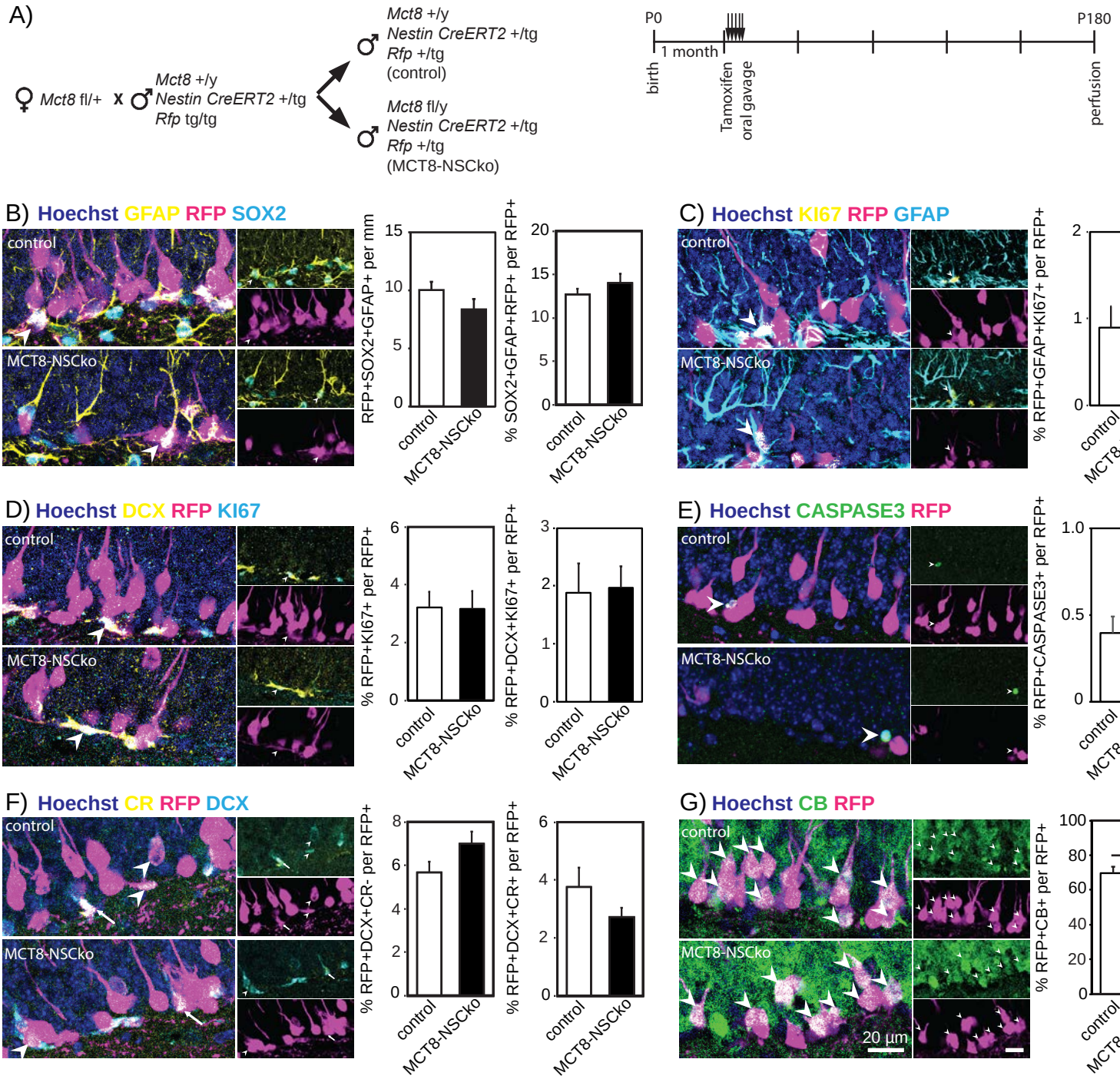
A)
♀ Mct8 fl/+ x ♂ Mct8 +/y
Nestin CreERT2 +/tg
Rfp tg/tg
♂ Mct8 +/y
Nestin CreERT2 +/tg
Rfp +/tg
(control)
♂ Mct8 fl/y
Nestin CreERT2 +/tg
Rfp +/tg
(MCT8-NSCko)
P0
P180
1 month
birth
Tamoxifen
oral gavage
perfusion
B) Hoechst GFAP RFP SOX2
control
MCT8-NSCko
RFP+SOX2+GFAP+ per mm
% SOX2+GFAP+RFP+ per RFP+
C) Hoechst KI67 RFP GFAP
% RFP+GFAP+KI67+ per RFP+
D) Hoechst DCX RFP KI67
% RFP+KI67+ per RFP+
% RFP+DCX+KI67+ per RFP+
E) Hoechst CASPASE3 RFP
% RFP+CASPASE3+ per RFP+
F) Hoechst CR RFP DCX
% RFP+DCX+CR- per RFP+
% RFP+DCX+CR+ per RFP+
G) Hoechst CB RFP
20 µm
% RFP+CB+ per RFP+
**

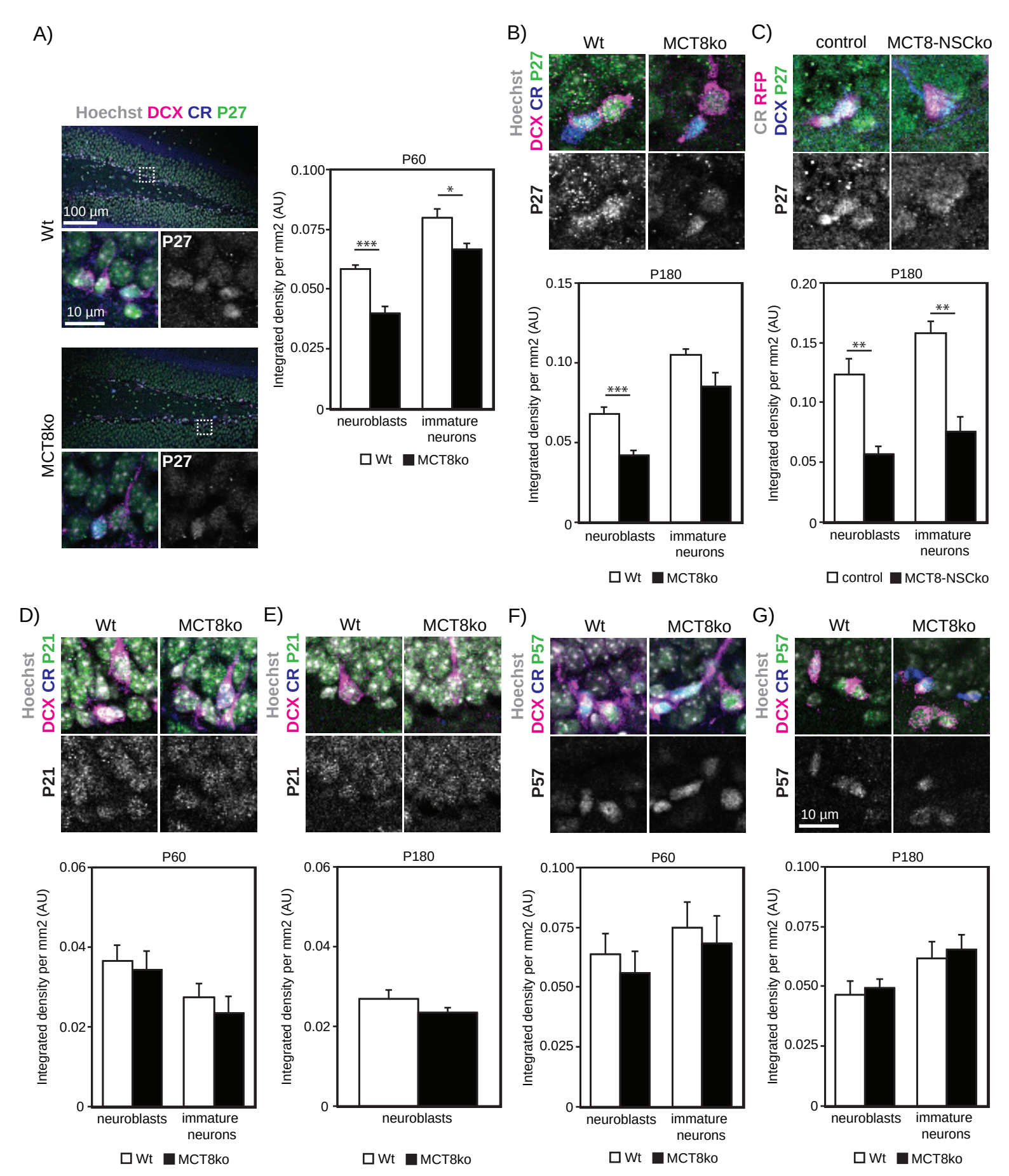
A)
Hoechst DCX CR P27
Wt
MCT8ko
100 µm
10 µm
P27
P60
Integrated density per mm2 (AU)
neuroblasts
immature neurons
Wt
MCT8ko
B)
Wt
MCT8ko
Hoechst DCX CR P27
P27
P180
C)
control
MCT8-NSCko
CR RFP DCX P27
P27
P180
control
MCT8-NSCko
D)
Hoechst DCX CR P21
P21
P60
E)
Hoechst DCX CR P21
P21
P180
F)
Hoechst DCX CR P57
P57
P60
G)
Hoechst DCX CR P57
P57
10 µm
P180